Self-consistent theory of orientational order and fluid–solid equilibria in weakly anisotropic fluids

Hyung-June Woo[a] and Xueyu Song
Department of Chemistry, Iowa State University, Ames, Iowa 50011

(Received 5 November 2001; accepted 28 December 2001)

A theoretical method of studying the effect of weak shape anisotropy on the freezing properties of classical fluids is discussed. A choice of an appropriate reference isotropic potential for a given general anisotropic model leads to the separation of the free energy into the part due to lattice formation, and the orientational correction. The reference free energy is calculated by applying the density functional theory. The anisotropic contribution to the free energy is treated by a self-consistent theory of orientational order. As an application, fluid–solid equilibria in the hard dumbbell model are considered. For the plastic crystal and the orientationally ordered phases of the hard dumbbell model, appropriate choices are made for the isotropic reference potential, density functional method is applied, and the resulting translational distribution of the molecular centers are utilized in the self-consistent calculation of the orientational ordering in the solid. The results obtained for the hard dumbbell fluids with various anisotropies are compared with the existing simulation data. © *2002 American Institute of Physics.* [DOI: 10.1063/1.1452111]

I. INTRODUCTION

Various aspects of the first-order phase transition from the homogeneous fluid phase into translationally ordered solid phases underlie many interesting phenomena observed in nature. Theoretical descriptions of such freezing transitions have been among the major challenges of modern statistical mechanics.[1] One of the important progresses in our understanding of the freezing transitions from the liquid phase point of view was the fact that, as in dense liquid, purely repulsive hard core interaction, and the associated packing effect, is the major driving force of freezing. The hard sphere fluid, with its well-characterized freezing properties,[2,3] thus serves as the canonical reference system for the studies of freezing transitions in isotropic fluids.

Recent progresses in our ability to model freezing phenomena analytically in such systems have been made possible by the successful application of the density functional theories.[4] In the original formulation, a solid phase with a regular lattice structure is viewed as a self-sustained inhomogeneous ''liquid,'' and thus treated by a perturbative approach with the homogeneous liquid phase as the reference system.[5,6] Well-known structural and thermodynamic properties of the homogeneous liquid serve as the input. Although quite successful, careful examination of the convergence properties of the perturbation expansion showed that attempts of systematic correction tend to spoil the results obtained within the second-order theory.[7]

As an alternative that avoids such difficulties, various forms of nonperturbative approaches collectively known as the weighted density approximations have been proposed.[8–11] The general idea consists of using the well-known homogeneous liquid properties such as the excess free energy and correlation functions, but at a coarse-grained effective liquid density. The effective density is generally much smaller than the physical density of the solid phase under consideration, justifying the use of the homogeneous liquid properties.

With such nonperturbative refinements, quantitative agreements with simulation results of the freezing transition of hard sphere fluid have now been achieved. To treat soft sphere fluid systems such as Lennard-Jones fluids, extensions of the thermodynamic perturbation theory[12,13] or adaptations of the integral equation methods[14–16] have been used.

Many of real molecular fluids or colloidal systems are more naturally modeled by anisotropic interaction potentials. The effects of such anisotropy on the phase behavior of classical fluids are most vividly seen in the appearances of the variety of liquid crystalline phases for highly anisotropic molecular and polymeric fluids.[17] Onsager's classic mean-field treatment of nematic ordering in infinitely long hard rods[18] provides an analogue of the canonical role played by the hard sphere phase behavior in the isotropic potential fluids. A systematic interpolation of the phase behavior of hard anisotropic fluids between the Onsager and the hard sphere limits has been achieved for the hard spherocylinder model through the Monte Carlo simulation study by Bolhuis and Frenkel.[19] Hard spherocylinder fluids consist of rigid cylinders of length L and diameter σ, each end-capped by a pair of hemispheres with the same diameter, which reduce to the hard sphere fluid for $L=0$. It was found that liquid crystalline phases appear for the reduced anisotropy parameter $L^*=L/\sigma \gtrsim 10$, with the Onsager result recovered naturally for the large L^* limit. For the $L^* \lesssim 1$ regime, on the other hand, it was observed that an orientationally disordered plastic crystal phase coexists with the fluid for small L^*, while an orientationally ordered phase becomes stable for larger anisotropies.

[a]Present address: Department of Chemical Engineering, University of Massachusetts, Amherst, MA 01002.

Such qualitative features in the weak anisotropy regime had also been observed in earlier Monte Carlo study of hard dumbbell fluids,[20–22] which consist of pairs of fused hard spheres with diameter σ and bond length L. In fact, by using appropriate rescaling of density units, the two model fluids were shown to have essentially the same phase behavior,[19,23] with a triple point delimiting the stability of the plastic phase at $L^* \simeq 0.4$, suggesting the generic nature of the trend observed.

It is in principle fairly straightforward to generalize the density functional formalisms used for the theories of freezing in isotropic fluids to examine such effects of weak anisotropy. The free energy is written as a functional of the local density, $\rho(\mathbf{r},\omega)$, which is defined as the number of molecules at position $\mathbf{r}$ with orientation ω. Functional derivatives of the free energy with the density yield the series of orientation-dependent direct correlation functions. Although many authors have considered such approaches on the second-order perturbative level for hard anisotropic models such as the hard dumbbell or hard spheroid fluids,[24–27] satisfactory results have been obtained only for relatively small anisotropy, $L^* \lesssim 0.1$.[20]

The major source of limitations of such approaches is presently not clear. It appears likely that nontrivial effects of anisotropy within the solid phase coexisting with fluid are not adequately captured by the conventional methods of density functional theory, which is based on using the homogeneous liquid phase as the reference. In particular, the relative stability of the plastic versus orientationally ordered phases would be governed by the subtle anisotropic packing effects inside the crystal, which would be mostly averaged out in the homogeneous fluid phases.

A simple phenomenological alternative to the density functional methods is the free volume, or the cell theory.[28] The free energy of the solid phase is assumed to be the logarithm of the free volume accessible to a particle confined inside a cage formed by its nearest neighbors fixed on their equilibrium positions. A good agreement of coexisting densities with simulation data is obtained when applied to the hard sphere solid.[3] Extensions of the cell theory have thus been applied successfully to the freezing in hard dumbbell fluids.[29,30]

As an attempt to incorporate the spirit of the cell theory into the well-defined and flexible formalisms of the density functional theories, we have recently presented a simple scheme of treating the fluid–solid equilibria in the weakly anisotropic model fluids.[31] Based on the separation of the given anisotropic potential into an isotropic reference part and the anisotropic remainder, the excess free energy of a solid phase is separated into two contributions, namely the free energy of formation of the regular lattice, and the orientational contribution. The former is calculated by an application of the conventional density functional methods, and a self-consistent mean-field treatment of the orientational ordering is utilized for the latter.

In the application of the method to the hard dumbbell freezing properties in Ref. 31, the hard sphere system with an effective diameter was used as the isotropic reference system, and the orientational free energy was calculated assuming a perfect localization of the translational degrees of freedom to the lattice sites. The translational and orientational parts of the free energy are not directly coupled in this approximation, and it is not obvious how the isotropic reference part should be chosen for the particular case under consideration. In addition, for the orientationally ordered phase, it was necessary to assume different lattice structures for the calculation of the translational and the orientational free energy contributions due to the neglect of the effect of imperfect localization on the solid phase free energy.

In the present paper, in addition to providing full details of the theoretical approach, we present results of calculations in which the above-mentioned difficulties are avoided by making a more appropriate choice of the reference potential for the phase under consideration, and allowing the translational degrees of freedom to fluctuate around the lattice sites in the orientational free energy calculations. The formalism of the free energy separation and the self-consistent theory of orientational ordering are reviewed in detail in the next section. The application of the method to the hard dumbbell freezing transitions is discussed in Sec. III. The final section contains discussions and conclusions.

II. FORMALISM

A. Free energy separation

We consider a classical molecular fluid with the potential energy

$$V[\{\mathbf{r}_i,\omega_i\}] = \frac{1}{2}\sum_{i\neq j}^{N} v(\mathbf{r}_i,\omega_i;\mathbf{r}_j,\omega_j), \tag{1}$$

where $\{\mathbf{r}_i,\omega_i\}$ is the set of molecular center coordinates and orientations, N is the total number of molecules, and $v(\mathbf{r}_i,\omega_i;\mathbf{r}_j,\omega_j)$ is the pairwise interaction potential between molecules i and j. The molecular orientations $\{\omega_i\}$ represent a set of angles (spherical coordinate angles θ and ϕ for linear molecules, and the three Euler angles for nonlinear molecules) with respect to a space-fixed coordinate system. The specific nature of the anisotropy present in the interaction potential need not be specified yet, but we do require the anisotropy to be relatively small: for example, for molecules with elongation anisotropy such as spheroids, spherocylinders, or dumbbells, the largest length parameter of a molecule is assumed not much larger than the shortest length parameter. In addition, we confine ourselves to short-ranged interactions, in which hard core interactions play a dominant role. Long-ranged potential models such as dipolar hard spheres are excluded.

The canonical partition function,

$$Z = \frac{1}{\Lambda^{3N}N!}\int d^N\mathbf{r}_i \int d^N\omega_i\, e^{-\beta V[\{\mathbf{r}_i,\omega_i\}]}, \tag{2}$$

where $1/\beta = k_B T$ is the Boltzmann constant times temperature, and Λ is the thermal wavelength, determines the Helmholtz free energy F by $\beta F = -\ln Z$. To achieve an effective separation of the translational and orientational free energy contributions, we separate the full interaction potential into an isotropic reference part and the anisotropic perturbation:

$$v(\mathbf{r}_i,\omega_i;\mathbf{r}_j,\omega_j)=v_0(r_{ij})+v_1(\mathbf{r}_i,\omega_i;\mathbf{r}_j,\omega_j), \tag{3}$$

where $r_{ij}=|\mathbf{r}_i-\mathbf{r}_j|$. The total potential energy is separated correspondingly as

$$V[\{\mathbf{r}_i,\omega_i\}]=V_0[\{\mathbf{r}_i\}]+V_1[\{\mathbf{r}_i,\omega_i\}] \tag{4}$$

with the obvious definitions analogous to Eq. (1). An appropriate choice of the isotropic reference potential would depend on the particular case under consideration, but in general should be chosen to closely mimic the homogeneous low density behavior of the full anisotropic fluids. The partition function can be rewritten as

$$Z=Z_0\langle e^{-\beta V_1[\{\mathbf{r}_i,\omega_i\}]}\rangle_0, \tag{5}$$

where Z_0 is the reference system partition function,

$$Z_0=\frac{1}{\Lambda^{3N}N!}\int d^N\mathbf{r}_i\int d^N\omega_i\, e^{-\beta V_0[\{\mathbf{r}_i\}]}$$

$$=\frac{\Omega^N}{\Lambda^{3N}N!}\int d^N\mathbf{r}_i\, e^{-\beta V_0[\{\mathbf{r}_i\}]} \tag{6}$$

with Ω the total area of solid angle elements. The angled brackets in Eq. (5) represent the average over the probability distribution of the reference system,

$$\langle\cdots\rangle_0\equiv\int d^N\mathbf{r}_i\,\mathcal{P}_0[\{\mathbf{r}_i\}]\int\frac{d^N\omega_i}{\Omega^N}(\cdots). \tag{7}$$

The translational probability distribution is given by

$$\mathcal{P}_0[\{\mathbf{r}_i\}]=\frac{e^{-\beta V_0[\{\mathbf{r}_i\}]}}{\int d^N\mathbf{r}_i\, e^{-\beta V_0[\{\mathbf{r}_i\}]}}. \tag{8}$$

For homogeneous liquid phases, partial reductions of the full phase space probability distribution (8) lead to various levels of reduced multiparticle distribution functions. The lowest level distribution, the single-particle density is constant, and the most important is the next lowest level distribution, which is proportional to the pair correlation function.

In contrast, for a crystalline solid phase, the distribution is dominated by the small neighborhood in the configurational space of the regular lattice structure. The single particle density with translational long range order accounts for most of the structural features contained in the full distribution function. The equilibrium single particle density is given by

$$\rho(\mathbf{r})=\langle\hat{\rho}(\mathbf{r})\rangle_0, \tag{9}$$

where $\hat{\rho}(\mathbf{r})$ is the microscopic density operator,

$$\hat{\rho}(\mathbf{r})=\sum_{i=1}^{N}\delta(\mathbf{r}-\mathbf{r}_i). \tag{10}$$

The functional form of the single-particle density used in the density functional theories, which has been shown to be highly accurate by comparisons with simulations, is the sum of Gaussians centered on the lattice sites

$$\rho(\mathbf{r})=\left(\frac{\alpha}{\pi}\right)^{3/2}\sum_{n=1}^{N}e^{-\alpha(\mathbf{r}-\mathbf{R}_n)^2}, \tag{11}$$

where $\{\mathbf{R}_n\}$ is the set of lattice vectors and α is the variational parameter representing the broadness of the lattice vibrations in the crystal. From Eq. (9), we obtain a form of the translational distribution function consistent with the parametrization (11):

$$\mathcal{P}_0[\{\mathbf{r}_i\}]=\left(\frac{\alpha}{\pi}\right)^{3N/2}\exp\left[-\alpha\sum_{i=1}^{N}(\mathbf{r}_i-\mathbf{R}_i)^2\right]. \tag{12}$$

It should be noted that unlike the single-particle density expression, Eq. (11), which is valid up to the homogeneous limit $\alpha=0$, the translational distribution Eq. (12) would be a good approximation only for a well-defined regular lattice structure with fairly large α.

Now from Eq. (5), the total free energy is written as

$$F=F_0+F_\omega, \tag{13}$$

where $F_0=-k_BT\ln Z_0$ and $F_\omega=-k_BT\ln Y_N$ with Y_N defined as

$$Y_N=\left\langle\int\frac{d^N\omega_i}{\Omega^N}e^{-\beta V_1[\{\mathbf{r}_i,\omega_i\}]}\right\rangle_\alpha$$

$$\equiv\int d^N\mathbf{r}_i\,\mathcal{P}_0[\{\mathbf{r}_i\}]\int\frac{d^N\omega_i}{\Omega^N}e^{-\beta V_1[\{\mathbf{r}_i,\omega_i\}]}. \tag{14}$$

Conventional methods of density functional theory can be applied to obtain the reference free energy, or the free energy of lattice formation, F_0, and furthermore to yield the Gaussian width parameter α, which completely determines the translational distribution function of the crystalline phase by Eq. (12).

B. Self-consistent theory of orientational order

The translational distribution function, Eq. (12), effectively results in the localization of the molecule i to the neighborhood of the lattice site $\mathbf{R}_i$, allowing for the use of lattice-based mean-field treatment of the orientational free energy contribution. A perfect localization is only achieved for $\alpha=\infty$, and for finite α, there exists in general a coupling between the two free energy contributions, F_0 and F_ω, through their dependences on α.

With the molecular centers localized to the neighborhood of regular lattice sites, a self-consistent method can be used to obtain the orientational correction to the free energy.[31] Neglecting interactions beyond nearest-neighbor distances on the lattice, Eq. (14) can be rewritten as

$$Y_N=\left\langle\int\frac{d^N\omega_n}{\Omega^N}\prod_{\langle n,m\rangle}Q_{nm}\right\rangle_\alpha, \tag{15}$$

where

$$Q_{nm}\equiv Q_{nm}(\mathbf{r}_n,\omega_n;\mathbf{r}_m,\omega_m)$$

$$=\exp[-\beta v_1(\mathbf{r}_n,\omega_n;\mathbf{r}_m,\omega_m)] \tag{16}$$

and the product runs over all of the pairs of molecules localized to the nearest-neighbor pairs of sites within the lattice. Since we aim at applications to hard core or near hard core

potentials, it is necessary to directly manipulate the Boltzmann factor Q_{nm} rather than the potential itself.

We consider the N-particle angular distribution function defined as

$$P_N^{(N)}[\{\omega_i\}]=\frac{1}{\Omega^N Y_N}\left\langle \prod_{\langle n,m\rangle} Q_{nm}\right\rangle_\alpha , \tag{17}$$

from which the series of k-particle reduced probability distributions are obtained by partial integrations

$$P_N^{(k)}[\{\omega_i^k\}]=\frac{1}{\Omega^N Y_N}\left\langle \int d^{N-k}\omega_n \prod_{\langle n,m\rangle} Q_{nm}\right\rangle_\alpha . \tag{18}$$

We now pick a particular lattice site 0 and consider the $k=1$ special case of Eq. (18) corresponding to the site,

$$p(\omega_0)\equiv P_N^{(1)}[\omega_0]$$

$$=\frac{1}{\Omega^N Y_N}\left\langle \int d^{N-1}\omega_n \prod_{\langle n,m\rangle} Q_{nm}\right\rangle_\alpha , \tag{19}$$

which we rewrite as

$$p(\omega_0)=\frac{1}{\Omega^N Y_N}\left\langle \int d^{n_c}\omega_n \prod_{n=1}^{n_c} Q_{0n} \times \int d^{N-n_c-1}\omega_m \prod_{\langle m,l\rangle'} Q_{ml}\right\rangle_\alpha . \tag{20}$$

In Eq. (20), the integrations have been separated into those over the molecules localized to the nearest-neighbor sites of the central site, and the rest of the sites. The second product excludes the pairs involving the central site. n_c denotes the number of nearest neighbors of a site within the lattice.

Equation (20) can be rewritten in terms of the n_c particle reduced distribution function of a new system that excludes the central site, which, from Eq. (18), is given by

$$P_{N-1}^{(n_c)}[\{\omega_i^{n_c}\}]$$

$$=\frac{1}{\Omega^{N-1}Y_{N-1}}\left\langle \int d^{N-n_c-1}\omega_n \prod_{\langle n,m\rangle'} Q_{nm}\right\rangle_\alpha . \tag{21}$$

To obtain a hierarchical relation between different levels of multiparticle distributions, we utilize the definition (21) to approximate Eq. (20) as

$$p(\omega_0)=\left\langle \int \frac{d^{n_c}\omega_n}{\Omega\xi}\prod_{n=1}^{n_c} Q_{0n}P_{N-1}^{(n_c)}[\{\omega_n^{n_c}\}]\right\rangle_\alpha , \tag{22}$$

where $\xi=Y_N^{1/N}$. Equation (22) becomes exact for $\alpha=\infty$.[31]

Equation (22) is the lowest member of the hierarchical relations connecting the single-particle distribution to the n_c particle distribution. As in any study of many body systems, a judicious choice of closure is crucial in the utilization of relations such as Eq. (22). In this paper, we employ one of the possible decoupling schemes in which the n_c particle angular distribution function is approximated as a simple product of the single-particle functions of the coordination shells

$$P_{N-1}^{(n_c)}[\{\omega_n^{n_c}\}]\simeq\prod_{n=1}^{n_c} p(\omega_n). \tag{23}$$

Combining Eqs. (22) and (23), we have

$$p(\omega_0)=\frac{1}{\Omega\xi}\left\langle \prod_{m=1}^{n_c}\int d\omega_1\, p(\omega_1)Q_{0m}(\mathbf{r}_0,\omega_0;\mathbf{r}_m,\omega_1)\right\rangle_\alpha . \tag{24}$$

Equation (24) can be solved by assuming a reasonable parametrized form of the single-particle distribution function, and using iterative methods to obtain a self-consistent solution. The orientational free energy per molecule, $f_\omega=F_\omega/N$ is determined by $f_\omega=-k_BT\ln\xi$.

III. FLUID–SOLID EQUILIBRIA

In this section we demonstrate an application of the formalism described above to the fluid–solid equilibria of hard dumbbell fluids. There exist a number of simple extensions of the hard sphere model with linear elongation anisotropy. The hard spherocylinder model has the advantage of allowing for the well-defined Onsager limit, $L^*\to\infty$, and the hard sphere limit, $L^*=0$. However, for the weak anisotropy regime $0<L^*<1$ to which we confine our attention in this paper, it has been shown that the hard spherocylinder model has essentially the same phase behavior as the hard dumbbell model.[19,23] The hard dumbbell model has the advantage of having a simpler overlap criterion, namely that of the four possible overlaps between the spheres of a pair of dumbbell molecules. It also allows for a straightforward generalization to the attractive interaction models via the use of the site–site interaction potentials.

The global phase behavior of the hard dumbbell model has been elucidated by Monte Carlo simulations. In contrast to the strong anisotropy regimes of the hard spherocylinder model in which various liquid crystalline phases are observed, the nontrivial effect of the orientational degrees of freedom manifests itself in the weak anisotropy regime as the existence of the orientational phase transition between the plastic crystal and the orientationally ordered solid phases. Singer and Mumaugh showed that the face-centered-cubic (fcc) plastic crystal phase is the stable solid phase only for bond lengths $L^*\lesssim 0.4$.[20] Subsequently, Monson and coworkers performed simulations of both the plastic crystal and the ordered solid phases of hard dumbbells with various bond length parameters, establishing a fairly complete phase diagram. It was shown that the fluid freezes into the plastic crystal phase for $L^*<0.38$, whereas it coexists with the ordered solid for $L^*>0.38$, for which the plastic phase is thermodynamically unstable.[21,22]

In this section, we apply the formalism developed in the preceding section to the fluid–solid equilibria of the hard dumbbell model, with the aim of demonstrating the utility of the theoretical method described above.

A. Density functional theory

The translational part of the free energy F_0 accounts for the contribution due to the formation of the regular lattice structure on which the self-consistent treatment of the orien-

tational ordering is based. Once an appropriate choice of the isotropic reference potential has been made, any of the well-established density functional methods for the freezing of isotropic model fluids can be used for the calculation of the translational free energy. In the present paper, we utilize the modified weighted density approximation (MWDA) first proposed by Denton and Ashcroft.[10] The MWDA has the advantage of being flexible and fairly successful for various hard and soft interaction potential models with moderate computational costs.

In the MWDA, the excess Helmholtz free energy per particle $f_{\mathrm{ex}}(\rho_s)$ of a solid phase with density ρ_s is approximated as the excess free energy $f_l(\hat{\rho})$ of the homogeneous liquid at an effective liquid density $\hat{\rho}$,[10]

$$f_{\mathrm{ex}}(\rho_s) \simeq f_l(\hat{\rho}). \tag{25}$$

The effective density is determined by the weighted average of the density profile $\rho(\mathbf{r})$ within the crystal,

$$\hat{\rho} = \frac{1}{N}\int d\mathbf{r}\, \rho(\mathbf{r}) \int d\mathbf{r}'\, \rho(\mathbf{r}')w(|\mathbf{r}-\mathbf{r}'|;\hat{\rho}), \tag{26}$$

where $N=\int d\mathbf{r}\,\rho(\mathbf{r})$ is the total number of particles. The weight function $w(r)$ in Eq. (26), satisfying the normalization condition, $\int d\mathbf{r}\, w(r)=1$, is determined by the requirement that the second functional derivative of the excess free energy with respect to density coincides with the direct correlation function in the homogeneous limit, which in the Fourier space leads to

$$-2\beta f_l'(\rho)\hat{w}(k;\rho) = c_l(k;\rho) + \delta_{k,0}\rho\beta f_l''(\rho), \tag{27}$$

where $c_l(k;\rho)$ is the second-order direct correlation function of the homogeneous liquid in k space, and the primes denote differentiations with respect to the density variable.

With the excess free energy per particle $f_l(\rho)$ and the direct correlation function $c_l(k;\rho)$ of the homogeneous liquid as the inputs, the effective weighted density $\hat{\rho}$ is determined by solving the self-consistent equation (26) with the weight function given by Eq. (27). The excess free energy is given by Eq. (25) with the weighted density thus obtained. Using the explicit parametrization of the single-particle density in the solid, Eq. (11), the equation that determines the weighted density can be written as

$$\hat{\rho} = \rho_s - \frac{\rho_s}{2\beta f_l'(\hat{\rho})}\sum_{\mathbf{k}\neq\mathbf{0}} e^{-k^2/2\alpha} c_l(k;\hat{\rho}), \tag{28}$$

where the summation is over the set of nonzero reciprocal lattice vectors of the lattice under consideration.

Recently, Khein and Ashcroft have reformulated the global weighted density approximation in a more general setting, which allows for substantial improvements of the predictions of the MWDA with essentially the same computational cost.[32] When specialized to the MWDA, it leads to a slight modification of Eq. (28) to

$$\gamma x = (\gamma-1)x^2 + 1 - \frac{(2-\gamma)}{2\beta f_l'(\hat{\rho})}\sum_{\mathbf{k}\neq\mathbf{0}} e^{-k^2/2\alpha} c_l(k;\hat{\rho}), \tag{29}$$

where $x=\hat{\rho}/\rho_s$, and $\gamma=1.1847$ is the parameter fixed by the requirement that the free energy expression satisfies the exact relation $\beta f_{\mathrm{ex}}=1$ in the zero-dimensional limit. With $\gamma=1$, Eq. (29) reduces to Eq. (28).

The total free energy of a solid phase is determined by the sum of the excess free energy and the ideal gas contribution,

$$\beta F_{\mathrm{id}}[\rho(\mathbf{r})] = N\beta f_{\mathrm{id}} = \int d\mathbf{r}\,\rho(\mathbf{r})[\ln\rho(\mathbf{r})\Lambda^3 - 1]. \tag{30}$$

For large values of the Gaussian overlap parameter $\alpha\sigma^2 \gtrsim 50$ relevant for the freezing transitions studied here, Eq. (30) is accurately approximated as the expression obtained by neglecting the overlap between the Gaussians,

$$\beta f_{\mathrm{id}}(\rho_s,\alpha) = \frac{3}{2}\ln\frac{\alpha}{\pi} - \frac{5}{2} + 3\ln\Lambda. \tag{31}$$

The translational free energy per molecule $f_0(\rho_s,\alpha)$ is given by

$$f_0(\rho_s,\alpha) = f_{\mathrm{id}}(\rho_s,\alpha) + f_{\mathrm{ex}}(\rho_s,\alpha). \tag{32}$$

B. Plastic crystal phase

The plastic crystal (PC) phase of the hard dumbbell model is characterized by the translational ordering into the fcc lattice without the orientational order. For the calculation of the free energy, it is necessary to identify the appropriate choice of the reference isotropic potential $v_0(r)$ in Eq. (3). In Ref. 31, an effective hard sphere model was used as the reference system for the calculation of the translational free energy. However, the use of a hard sphere model with diameter $d>\sigma$ as the reference leads to the difficulty in identifying the corresponding anisotropic potential $v_1(\mathbf{r}_i,\omega_i;\mathbf{r}_j,\omega_j)$ in Eq. (3). For imperfect localization of the translational distribution characterized by a finite α in Eq. (12), $v_1(\mathbf{r}_i,\omega_i;\mathbf{r}_j,\omega_j)=-\infty$ for some of the configurational space.

An appropriate choice of the isotropic reference potential for the PC phase avoiding such difficulty can be provided by the reference average Mayer (RAM) potential, which is defined as

$$-\beta v_0(r) = \ln\int\frac{d\omega_i}{\Omega}\int\frac{d\omega_j}{\Omega} e^{-\beta v_1(\mathbf{r}_i,\omega_i;\mathbf{r}_j,\omega_j)}. \tag{33}$$

For the hard dumbbell potential, a simple analytic expression[33] that smoothly connects the two regions $v_0(r)=\infty$ for $r/\sigma<[1-(L^*)^2/2]^{1/2}$ and $v_0(r)=0$ for $r/\sigma>L^*+1$ is available.

The application of the density functional theory to the reference fluid with the RAM potential requires the excess free energy and the direct correlation function of the homogeneous fluid. We employ the modified hypernetted-chain equation (MHNC) method[34] to calculate the thermodynamic and structural properties of the RAM potential reference fluid. The combination of the MHNC and MWDA has been successfully used to obtain the phase behavior of various short-ranged soft potential model systems such as the repulsive power-law potential,[14] $2n$-n potential,[16] and C_{60}.[15,35]

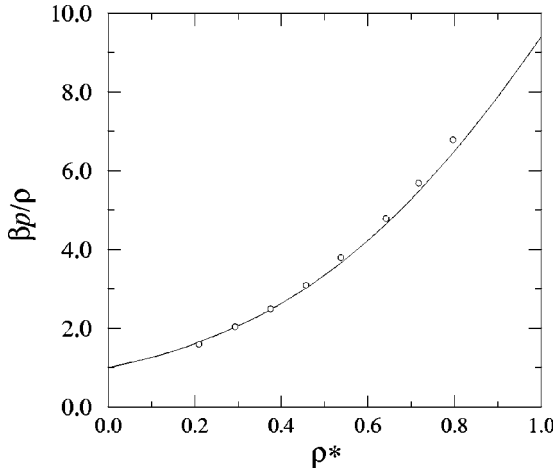

FIG. 1. $\beta p/\rho$ vs ρ^* of the hard dumbbell RAM potential fluid with $L^*=0.6$. The solid line is from the MHNC solution. Circles are the simulation data from Ref. 33.

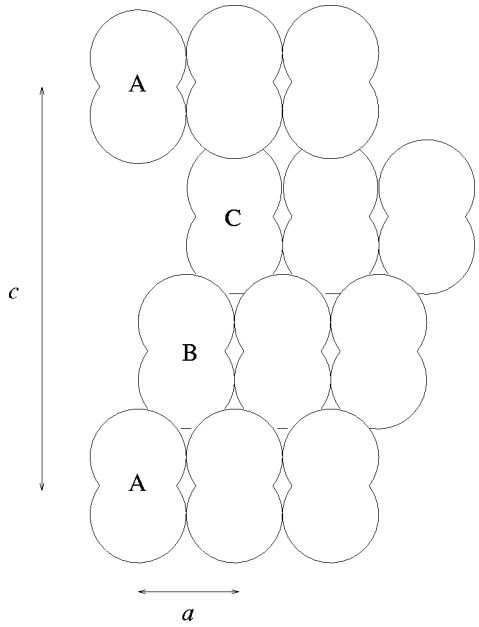

FIG. 2. ABC stacking of hexagonal layers of dumbbells.

The MHNC consists of the iterative solution of the Ornstein–Zernike relation with the modified hypernetted-chain closure,

$$g_l(r)=\exp[-\beta v_0(r)+g_l(r)-1-c_l(r)+B(r,\overline{\sigma})], \tag{34}$$

where $g_l(r)$ is the pair correlation function of the fluid, and $B(r,\overline{\sigma})$ is the bridge function of an effective hard sphere system with diameter $\overline{\sigma}$. The hard sphere diameter $\overline{\sigma}$ is determined by the thermodynamic consistency condition,

$$\frac{\partial \beta p}{\partial \rho}=1/\rho k_B T\kappa, \tag{35}$$

where p is the virial pressure, and κ is the isothermal compressibility.

We have applied the MHNC method to the hard dumbbell RAM potential fluid to obtain the pressure and direct correlation function as functions of density. The excess free energy was obtained by the thermodynamic integration of the pressure data with respect to density,

$$\beta f_l(\rho)=\int_0^{\rho} d\rho' \left[\frac{\beta p(\rho')}{\rho'}-1\right]. \tag{36}$$

The direct correlation function in Fourier space and the excess free energy data for a range of density values from the solution of the MHNC equations were stored, and subsequently used for the iterative solution of the MWDA equation (29) with numerical interpolations in density and k space. Figure 1 shows the comparison of the calculated pressure as a function of the reduced density ρ^* of the RAM potential fluid with the Monte Carlo simulation data from Ref. 33. The reduced density is defined as $\rho^*=\rho d^3$, where $d=\sigma[1+3L^*/2-(L^*)^3/2]^{1/3}$ is the diameter of the sphere whose volume is equal to the hard dumbbell of bond length L, such that $\eta=\pi\rho^*/6$ is equal to the packing fraction of the dumbbell. It allows for the direct comparison with the hard sphere limit of the same packing fraction.

For the density functional as well as the orientational free energy calculations, it is necessary to assume a certain crystal symmetry for the solid phase under consideration. Extrapolating from the hard sphere limit in which the fcc crystal phase is known to be stable, it is natural to assume fcc symmetry for the PC phase of hard dumbbell solids, as was done in the simulation studies of hard dumbbell and spherocylinder models. In the present paper, we consistently consider the crystal symmetries of both PC and OS phases based on the ABC stacking of the hexagonal layers of dumbbells (Fig. 2).

Given the lattice constant ratio $R=c/a$ of the underlying simple hexagonal lattice, the bulk density of the solid ρ_s determines the lattice constants by $a=(6/\sqrt{3}\rho_s R)^{1/3}$. For the orientationally disordered PC phase, the dumbbells in each hexagonal layers are freely rotating with their molecular centers anchored on the hexagonal lattice points. The lattice constant ratio for the stable PC phase is therefore expected to be the ideal value, $R=\sqrt{6}$, obtained by replacing the dumbbells in Fig. 2 with spheres. The lattice becomes equivalent to the simple fcc in this case, with the lattice vector **c** in Fig. 2 along the [111] direction of the cubic unit cell.

The OS phases would instead be characterized by the lattice constant ratio larger than the ideal value. Bolhuis and Frenkel showed in their Monte Carlo simulation study of the hard spherocylinder model that such an ABC-stacked solid phase is stable for high densities for $L^*\lesssim 10$.[19] For the hard dumbbells, due to the concave region of the molecular surface near the molecular center, a slightly more efficient packing is achieved by tilting the molecular axes towards the **a** $+$**b** direction. The resulting distorted lattice structures with different packing sequences of the hexagonal layers were considered in the simulation studies of Monson and co-workers.[21,22] However, the maximum packing density of the undistorted ABC structure remains only slightly lower than that of the distorted structure for bond lengths up to

$L^*<0.8$. The close agreement of the phase diagrams of the hard spherocylinder and hard dumbbell models from simulations[19,23] further suggests that the enhanced packing effect of tilting the molecular axes for dumbbells is moderate at best, and we therefore confine our studies in this paper to the undistorted ABC-stacked structure for simplicity.

To calculate the orientational contribution to the free energy, a parametrized form of the single-particle orientational distribution function is used to find the solution of Eq. (24). With the laboratory coordinate system fixed such that the x, y, and z axes coincide with the $\mathbf{a}$, $\mathbf{b}-\mathbf{a}/2$, and $\mathbf{c}$ direction of the hexagonal lattice in Fig. 2, the preferred direction of the dumbbell molecular axes would be in the z direction, or $\theta=0$ in the spherical coordinate system. We therefore use the following form of the orientational distribution function:

$$p(\omega)=p(\theta)=A^{-1}\exp(b\cos^2\theta), \tag{37}$$

where A is the normalization factor. A nonzero value of b signifies the orientational ordering in the preferred direction $\theta=0$. A bounded orientational order parameter $0\leqslant q\leqslant 1$ can be defined as

$$q=\int d\omega\, p(\omega)P_2(\cos\theta)=\frac{1}{2}\left[\frac{3z_2(b)}{z_0(b)}-1\right], \tag{38}$$

where $P_2(x)=(3x^2-1)/2$ and

$$z_n(b)=\int_0^1 dx\, x^n\exp(bx^2). \tag{39}$$

Equation (24) can now be rewritten as a set of two self-consistent equations,

$$\xi=\left\langle \int\frac{d\omega_0}{4\pi}\prod_{m=1}^{n_c}\int d\omega_1\, p(\omega_1)Q_{0m}\right\rangle_\alpha, \tag{40a}$$

$$q=\left\langle \int\frac{d\omega_0}{4\pi\xi}P_2(\cos\theta_0)\prod_{m=1}^{n_c}\int d\omega_1\, p(\omega_1)Q_{0m}\right\rangle_\alpha, \tag{40b}$$

obtained by integrating the left-hand side of Eq. (24) with respect to ω_0, without and with the weight $P_2(\cos\theta_0)$, respectively. To solve Eqs. (40), one can start with an initial guess of b, calculate ξ by Eq. (40a), calculate q by Eq. (40b), invert Eq. (38) to find a refined value of b, and continue until convergence is achieved.

While the angular integrals in Eqs. (40) can be easily calculated by Gaussian quadratures, the averages over the translational distribution involved in Eqs. (40) are $3(n_c+1)$-dimensional integrals, and the direct evaluation is not feasible. We therefore separate the averages over the orientational and the translational degrees of freedom by first solving the self-consistent equations for a fixed set of molecular centers,

$$\xi[\mathbf{r}_m]=\int\frac{d\omega_0}{4\pi}\prod_{m=1}^{n_c}\int d\omega_1\, p(\omega_1)Q_{0m}(\mathbf{r}_0,\omega_0;\mathbf{r}_m,\omega_1),$$

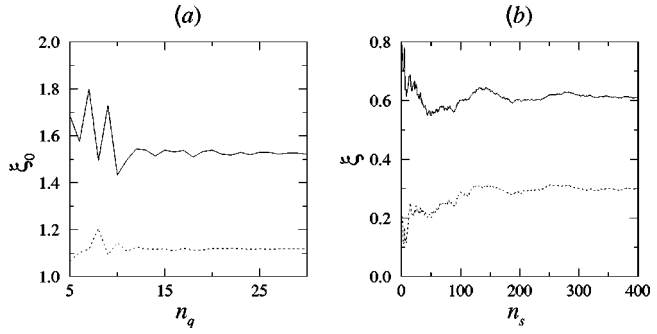

FIG. 3. Convergences of (a) ξ_0 for $\alpha=\infty$ with the increasing number n_q of points used in the quadrature in each angular dimension; and (b) of ξ with respect to the increasing number n_s of sets of the molecular center coordinates sampled over the Gaussian distribution, Eq. (12). The bond length is $L^*=0.3$, and the solid and dotted lines are for $\rho^*=1.0$ and $\rho^*=1.1$, respectively. The order parameter remains as $q=\mathcal{O}(10^{-3})$ for both cases. In (b), $\alpha\sigma^2=100$ and $n_q=20$.

$$q[\mathbf{r}_m]=\int\frac{d\omega_0}{4\pi\xi[\mathbf{r}_m]}P_2(\cos\theta_0)\times\prod_{m=1}^{n_c}\int d\omega_1\, p(\omega_1)Q_{0m}(\mathbf{r}_0,\omega_0;\mathbf{r}_m,\omega_1), \tag{41}$$

and sampling the results over the Gaussian distribution of molecular centers around the lattice sites:

$$\xi=\langle\xi[\mathbf{r}_m]\rangle_\alpha, \tag{42a}$$

$$q=\langle q[\mathbf{r}_m]\rangle_\alpha. \tag{42b}$$

The integrand in Eqs. (41) given by Eq. (16) can be rewritten as

$$Q_{0m}(\mathbf{r}_0,\omega_0;\mathbf{r}_m,\omega_1)=e^{\beta v_0(r_{0m})}\Delta(\mathbf{r}_0,\omega_0;\mathbf{r}_m,\omega_1), \tag{43}$$

where $r_{0m}=|\mathbf{r}_0-\mathbf{r}_m|$ and $\Delta(\mathbf{r},\omega,\mathbf{r}',\omega')=1$ if the pair of dumbbells at $\mathbf{r}$ and $\mathbf{r}'$ with orientations ω and ω' do not overlap, and zero otherwise. The overlap can easily be checked by calculating the distances between the four possible combinations of the dumbbell spheres. In addition, the isotropic prefactor in Eq. (43), independent of angles, needs to be kept only during the average involved in Eq. (42a).

The Gauss–Legendre quadrature was used to calculate the angular integrals in Eqs. (41). Figure 3 shows the convergence of $\xi_0=\xi[\mathbf{R}_m]$ for $L^*=0.3$ with the increasing number n_q of points used in the quadrature, as well as that of ξ obtained by the average over the translational distribution of the coordination dumbbells, Eqs. (42) with the number n_s of sets of coordinates $\{\mathbf{R}_m\}$. It is seen that the inclusion of the finite width of the Gaussian distribution of molecular centers leads to the smaller value of ξ, or an increase in the orientational free energy.

The total free energy per molecule of the PC phase can now be obtained by adding the translational free energy of the RAM potential fluid from the MWDA and the orientational part, and minimizing the sum with respect to the Gaussian width parameter α. The reduced free energy density $\rho^*\beta f$ as a function of density for a number of bond lengths is shown in Fig. 4, along with the fitting into a cubic polynomial of the data. In the reduced unit, the free energy

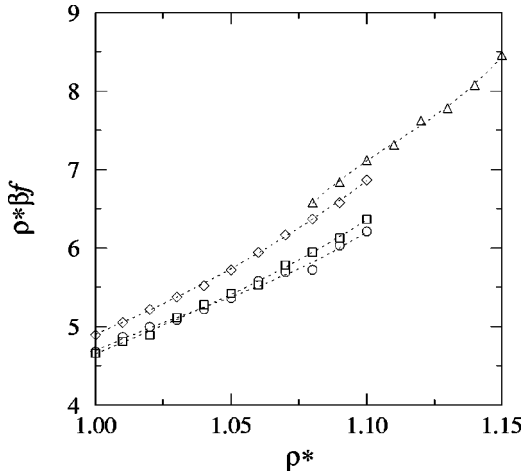

FIG. 4. The total reduced free energy density $\rho^*\beta f$ of the PC phase as a function of the reduced density. The circles, squares, diamonds, and triangles are the results of the calculations for $L^*=0.1$, 0.2, 0.3, and 0.35, respectively. The dotted lines are the polynomial fits to the data. $n_q=20$ and $n_s \geqslant 200$ for each cases.

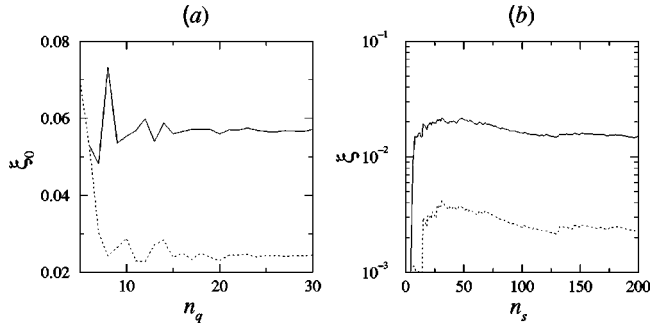

FIG. 5. Convergences of (a) ξ_0 for $\alpha=\infty$ for the OS phase with respect to n_q; and (b) ξ with respect to n_s for $L^*=0.4$. The solid and dotted lines are for $\rho^*=1.2$ and 1.3, respectively. $\alpha\sigma^2=400$ for (b), and $R=R_{\mathrm{cp}}$ for both cases.

of the PC phase for a given density remains nearly the same for $L^* \lesssim 0.2$, and begins to increase sharply for $L^* \gtrsim 0.3$. For $\rho^* \gtrsim 1.1$, the weighted density of the RAM fluid required in the MWDA calculation becomes high enough that the MHNC iteration ceases to converge, limiting the accessible range of calculation for the PC phase.

C. Orientationally ordered solid

For bond lengths $L^*>0.4$, the fluid freezes directly into the orientationally ordered solid (OS) phase. The lattice structure of the OS phase is characterized by the same ABC-stacked hexagonal structure depicted in Fig. 2, but with the nonideal lattice constant ratio $R>\sqrt{6}$. A simple geometric consideration of the close-packed ABC structure in Fig. 2 yields the maximum R value as $R_{\mathrm{cp}}=\sqrt{6}+3L^*$. In fact, for the OS phase with a high degree of orientational ordering ($q \simeq 1$), the lattice constant ratio is expected to be close to the close-packing value, as has been observed in the simulations.[21] Therefore, the lattice constant ratio enters the free energy calculation as an additional variable, and the free energy would have a second minimum in R near the close-packing value. As in the PC phase, the iterative solution of the Eqs. (41), and the subsequent averaging over the translational distribution, yield the values of the self-consistent orientational free energy and the order parameter.

To estimate the translational free energy contribution, a choice of the isotropic reference potential appropriate for the OS phase has to be made. In principle, since the reference potential also affects the value of the orientational free energy as well through the prefactor of Eq. (43), the total free energy should not depend very much on the different choices of the isotropic reference system, and any sensible choice including the RAM potential used for the PC phase would work. In practice, however, the density functional calculation relies on the existence of the effective homogeneous liquid approximating the solid phase of the chosen reference model system. The iteration of the self-consistent determination of weighted density in the MWDA was found not to converge for R near the close-packing value, suggesting the absence of the effective liquid density corresponding to the hexagonal lattice with large vertical distortions.

A more appropriate isotropic reference system for the OS phase with the degree of orientational ordering close to its maximum ($q \simeq 1$) is the hard sphere system with diameter $\bar{\sigma}=\sigma$, which is the contact distance between a pair of dumbbells within a hexagonal plane with perfect ordering of their molecular orientations (Fig. 2). We therefore use the hard sphere system as the isotropic reference for the OS phase. The anisotropic part of the potential can be replaced by the total hard dumbbell potential in this case (ignoring the concave region of the surface around the molecular center).

Figure 5 shows the convergence of the $\xi[\mathbf{R}_m]$ with respect to the number of points in the angular quadrature n_q. Convergence of the iterations involved in solving Eqs. (41) is very fast, and in general, less than five iterations were needed both for the PS and OS phases for a given set of $\{\mathbf{R}_m\}$. As shown in Fig. 6, the order parameter q increases monotonically from zero as R increases. As in the PC phase, the effect of lattice vibrations on the free energy of the OS phase is included by α average, Eqs. (42) (Fig. 5). The resulting ξ

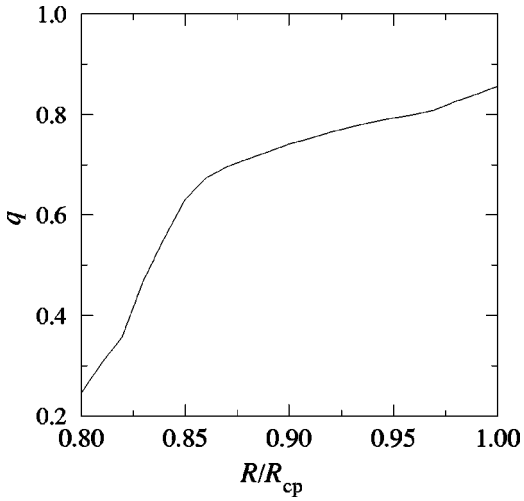

FIG. 6. The orientational order parameter q as a function of the lattice constant ratio R for $L^*=0.4$, $\rho^*=1.2$, $n=20$, and $\alpha=\infty$. $R_{\mathrm{cp}}=3.65$ in this case.

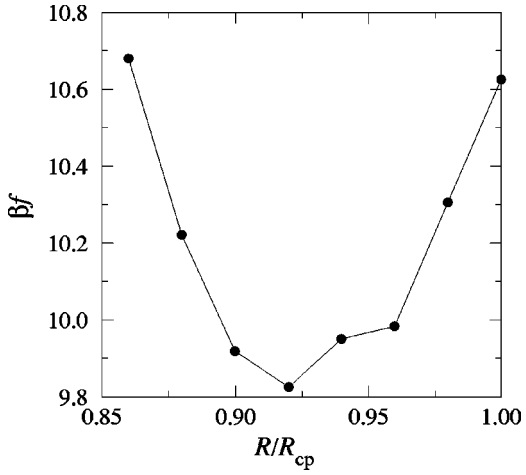

FIG. 7. The R dependence of the free energy per molecule for the OS phase with $L^*=0.4$. $n_q=20$, $n_s=100$ for the calculation of f_ω. $R_{cp}=3.65$ in this case.

values are generally orders of magnitude smaller than those in the PC phase, and the relative magnitude of the orientational free energy for an OS phase is much larger than in the PC phase.

For the calculation of the free energy of an OS phase, f_0 was obtained for given R and α, f_ω calculated by the average over the translational distribution given by α was added, and the sum was minimized with respect to R and α. The R dependence of the free energy is illustrated in Fig. 7, where a free energy minimum is shown to exist near the close-packing value. The resulting free energy density of the OS phase is shown for three different bond length parameters in Fig. 8.

D. Phase equilibria

Fluid–solid phase coexistence densities can be obtained from the free energy density data by the conditions of equality of pressure and chemical potential. Fluid-PC and fluid-OS phase coexistence densities were calculated by taking derivatives of the polynomial fits to the solid free energy densities, and utilizing the empirical equation of state for the fluid phases.[36]

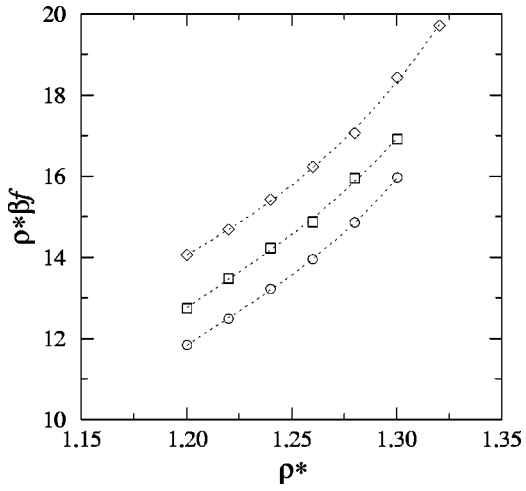

FIG. 8. The total reduced free energy density $\rho^*\beta f$ of the OS phase as a function of the reduced density. The circles, squares, and diamonds are the results of the calculations for $L^*=0.4$, 0.5, and 0.6, respectively. $n_q=20$ and $n_s=100$ for each cases. The dotted lines are the polynomial fits to the data.

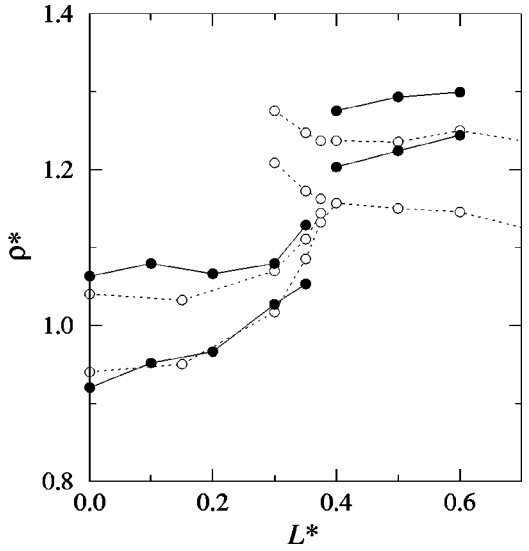

FIG. 9. Phase diagram of hard dumbbell fluids. Filled circles are the calculated coexistence densities. Open circles are the simulation results from Refs. 21 and 22.

Fluid-PC coexistence densities obtained, as shown in Fig. 9, agrees well with existing simulation results. In particular, with the simplified treatment of Ref. 31, the coexistence regions for $L^*\lesssim 0.2$ values had been found to be broadened compared to the simulation results, mainly due to the neglect of the coupling between the translational and orientational free energy contributions. The present approach more properly accounts for the effect of the imperfect localization of the molecular centers in the PC phase, resulting in the better agreement with simulations for low anisotropy regimes. The PC phase were found to become unstable for $L^*\gtrsim 0.4$. For bond length range $0.35<L^*<0.4$, the difference between the free energy densities for the PC and fluid phases becomes of the same order of magnitude as the statistical errors associated with the α average, making the determination of coexistence properties difficult.

The fluid-OS coexistence densities obtained are seen to be larger than those of simulation data. Possible origins of the error might include the stabilizing effect of tilting the molecular axes of dumbbells relative to the c direction in the OS phase, which was neglected in our study, and the limitation of the particular choice of the isotropic reference system. In addition, the MWDA method used for the translational free energy calculation ceases to converge for large anisotropy regimes, $L^*\gtrsim 0.6$.

IV. CONCLUDING REMARKS

The approach presented in this paper constitutes an alternative method to extend the density functional theories of freezing to systems characterized by anisotropic interaction potentials. The effective localization of the molecular centers in the solid phases is exploited to allow the use of lattice-

based self-consistent method to calculate the anisotropic contributions to the free energy. Many directions for generalizations and refinements are possible, including the treatments of nonlinear molecules and applications to the phase behavior of colloidal systems and proteins.

Apart from the general formalism, the success of a particular application of the method, including the calculations reported here, would strongly depend on the quality of input data. The efficiency of the translational free energy calculations done by the density functional methods imposes limitations on the applicability of the present approach. Due to the rather limited range of convergence of the weighted-density approximations, the OS phase coexistence calculations had to be limited to small anisotropies only. It would be worthwhile to pursue improvements by utilizing alternative methods, such as the fundamental measure approach of density functional theory,[37] which does not require the existence of the effective liquid phase.

ACKNOWLEDGMENT

The authors are grateful for the partial financial support by a Petroleum Research Fund, administrated by American Chemical Society.

[1] D. W. Oxtoby, Nature (London) **347**, 725 (1990).
[2] B. J. Alder and T. E. Wainwright, J. Chem. Phys. **27**, 1208 (1957).
[3] W. G. Hoover and F. H. Ree, J. Chem. Phys. **49**, 3609 (1968).
[4] R. Evans, in *Fundamentals of Inhomogeneous Fluids*, edited by D. Henderson (Dekker, New York 1992).
[5] T. V. Ramakrishnan and M. Yusouff, Phys. Rev. B **19**, 2775 (1979).
[6] A. D. J. Haymet and D. W. Oxtoby, J. Chem. Phys. **74**, 2559 (1981).
[7] W. A. Curtin, J. Chem. Phys. **88**, 7050 (1988).
[8] P. Tarazona, Mol. Phys. **52**, 81 (1984).
[9] W. A. Curtin and N. W. Ashcroft, Phys. Rev. A **32**, 2909 (1985).
[10] A. R. Denton and N. W. Ashcroft, Phys. Rev. A **39**, 4701 (1989).
[11] J. F. Lutsko and M. Baus, Phys. Rev. A **41**, 6647 (1990).
[12] W. A. Curtin and N. W. Ashcroft, Phys. Rev. Lett. **56**, 2775 (1986).
[13] L. Mederos, G. Navascués, and P. Tarazona, Phys. Rev. E **49**, 2161 (1994).
[14] B. B. Laird and D. M. Kroll, Phys. Rev. A **42**, 4810 (1990).
[15] C. Caccamo, Phys. Rev. B **51**, 3387 (1995).
[16] M. Hasegawa and K. Ohno, J. Phys.: Condens. Matter **9**, 3361 (1997).
[17] P. G. de Gennes and J. Proust, *The Physics of Liquid Crystals* (Oxford, New York, 1993).
[18] L. Onsager, Ann. N.Y. Acad. Sci. **51**, 627 (1949).
[19] P. Bolhuis and D. Frenkel, J. Chem. Phys. **106**, 666 (1997).
[20] S. J. Singer and R. Mumaugh, J. Chem. Phys. **93**, 1278 (1990).
[21] C. Vega, E. P. A. Paras, and P. A. Monson, J. Chem. Phys. **96**, 9060 (1992).
[22] C. Vega, E. P. A. Paras, and P. A. Monson, J. Chem. Phys. **97**, 8543 (1992).
[23] C. Vega and P. A. Monson, J. Chem. Phys. **107**, 2696 (1997).
[24] J. D. McCoy, S. J. Singer, and D. Chandler, J. Chem. Phys. **87**, 4853 (1987).
[25] J. F. Marko, Phys. Rev. Lett. **60**, 325 (1988).
[26] S. J. Smithline, S. W. Rich, and A. D. J. Haymet, J. Chem. Phys. **88**, 2004 (1988).
[27] U. P. Singh, U. Mohanty, and Y. Singh, Phys. Rev. A **38**, 4377 (1988).
[28] J. E. Lennard-Jones and A. F. Devonshire, Proc. R. Soc. London, Ser. A **168**, 53 (1937).
[29] E. P. A. Paras, C. Vega, and P. A. Monson, Mol. Phys. **77**, 803 (1992).
[30] S. C. Gay, J. C. Rainwater, and P. D. Beale, J. Chem. Phys. **112**, 9841 (2000).
[31] H.-J. Woo and X. Song, Phys. Rev. E **63**, 051501 (2001).
[32] A. Khein and N. W. Ashcroft, Phys. Rev. Lett. **78**, 3346 (1997); Phys. Rev. E **60**, 2875 (1999).
[33] F. Koher, N. Quirke, and J. W. Perram, J. Chem. Phys. **71**, 4128 (1979).
[34] Y. Rosenfeld and N. W. Ashcroft, Phys. Rev. A **20**, 1208 (1979).
[35] M. Hasegawa and K. Ohno, Phys. Rev. E **54**, 3928 (1996).
[36] D. J. Tildesley and W. B. Streett, Mol. Phys. **41**, 85 (1980).
[37] Y. Rosenfeld, M. Schmidt, H. Löwen, and P. Tarazona, Phys. Rev. E **55**, 4245 (1997).